

that we designed for preferential absorption of chemical nerve agents. HC is an acidic, strong-hydrogen-bonding polycarbosilane (25). We coated a sensor with a thin layer (~ 100 nm) of HC and tested the response to several analytes. The response of this polymer-coated sensor to repeated 10-s doses of acetone ranging from 60 to 540 ppm is shown in Fig. 4. The acetone produces a large, rapid response that is ~ 100 times larger than the response measured in the same sensor before the HC deposition. The HC concentrates the acetone vapor in the vicinity of the SWNTs, which increases the response while maintaining a rapid response time. The response to a single 200-s dose of DMMP delivered at 320 ppb shows that the measured gain for DMMP relative to the uncoated sensor is about 500 (Fig. 4). Note that the low diffusion rate of DMMP in the HC causes a slower recovery rate, $t_{90} = 370$ s. For water and chloroform, the polymer coating produces much lower response gains of 1 and 10, respectively. Thus, the HC provides a large chemically selective gain, demonstrating the feasibility of SWNT sorption-based chemical sensing.

These sensor characteristics compare favorably with those of commercial chemicapacitors. Using a signal-to-noise ratio of 3:1 as a detection criterion, we estimate that MDL = 0.5 ppm and $t_{90} < 4$ s for acetone and MDL = 0.5 ppb and $t_{90} = 370$ s for DMMP. For these same analytes, the commercial sensor achieves a MDL = 2 ppm and $t_{90} = 228$ s for acetone and MDL = 2 ppb and $t_{90} = 3084$ s for DMMP (4). We attribute our faster response and recovery times to the use of a much thinner layer of chemoselective material. For HC, the minimum layer thickness was limited by the tendency of the HC to form a discontinuous film below ~ 100 nm.

Our initial polymer-coated SWNT sensors achieve both higher sensitivity and faster response times than do current chemicapacitors. However, both of these properties can be substantially improved with a few design modifications. The sensitivity is currently limited by the small series capacitance of the thick SiO₂ layer. By thinning the SiO₂ layer or replacing it with a high-dielectric constant insulator (28), we estimate that we can increase the series capacitance by about a factor of 10, which should produce a comparable increase in response.

The response time for analytes such as DMMP is limited by diffusion through the layer of HC. Because the SWNT capacitor is based on a surface effect, we can improve the response time and still achieve chemical gain by using extremely thin layers of chemoselective material down to, and including, a single molecular monolayer.

To explore this limit of a chemoselective monolayer, we coated the SiO₂ surface with a self-assembled monolayer (SAM) of

allyltrichlorosilane. We then reacted the terminal alkenes with hexafluoroacetone to produce a monolayer of hexafluoroisopropanol that partially covers the SWNTs with fluoroalcohol groups. The response of this SAM-coated sensor to repeated 10-s doses of DMMP ranging from 320 ppb to 2.9 ppm is shown in Fig. 4. For this sensor, the response tracks our vapor-delivery system, indicating that $t_{90} < 4$ s, and we measured a MDL = 50 ppb. Notably, with the SAM coating, the capacitance response of DMMP relative to that of water is increased by a factor of 40, indicating that we achieved substantial chemically selective gain. These initial promising results indicate that optimization of the chemoselective monolayers to better cover the SWNTs, combined with improved sensor design, can result in a new class of sorption-based sensors that combine the features of low power, high sensitivity, and fast response time.

References and Notes

1. R. A. McGill *et al.*, *Sens. Actuators B* **65**, 10 (2000).
2. J. W. Grate, B. M. Wise, M. H. Abraham, *Anal. Chem.* **71**, 4544 (1999).
3. H. T. Nagle, S. S. Schiffman, R. Gutierrez-Osuna, *IEEE Spectr.* **35**, 22 (1998).
4. S. V. Patel *et al.*, *Sens. Actuators B* **96**, 541 (2003).
5. G. Delapierre, H. Grange, B. Chambaz, L. Destannes, *Sens. Actuators* **4**, 97 (1983).
6. A. Hierlemann *et al.*, *Sens. Actuators B* **70**, 2 (2000).
7. M. P. Eastman *et al.*, *J. Electrochem. Soc.* **146**, 3907 (1999).
8. M. C. Lonergan *et al.*, *Chem. Mater.* **8**, 2298 (1996).
9. J. R. Li, J. R. Xu, M. Q. Zhang, M. Z. Rong, *Carbon* **41**, 2353 (2003).
10. E. S. Snow, J. P. Novak, P. M. Campbell, D. Park, *Appl. Phys. Lett.* **82**, 2145 (2003).
11. E. S. Snow, P. M. Campbell, J. P. Novak, *Appl. Phys. Lett.* **86**, 033105 (2005).
12. D. R. Lide, *CRC Handbook of Chemistry and Physics* (CRC Press, Boca Raton, FL, ed. 75, 1995), pp. 15-43-15-49.
13. G. M. Kosolapoff, *J. Chem. Soc.* 3222 (1954).

14. J. D. Jackson, *Classical Electrodynamics* (Wiley, New York, ed. 2, 1975), pp. 155-158.
15. S. Brunauer, P. H. Emmett, E. Teller, *J. Am. Chem. Soc.* **60**, 309 (1938).
16. Density functional calculations of adsorbates on graphene sheets in uniform electric fields were performed using the generalized-gradient approximation and the Perdue, Burke, Ernzerhof parameterization of exchange and correlation in the Gaussian 03 localized-basis package (Gaussian 03, Revision C.02; M. J. Frisch *et al.*, Gaussian, Inc., Pittsburgh PA, 2003).
17. J. H. Walther, R. Jaffe, T. Halicioglu, P. Koumoutsakos, *J. Phys. Chem. B* **105**, 9980 (2001).
18. J. Kong *et al.*, *Science* **87**, 622 (2000).
19. L. Valentini *et al.*, *Appl. Phys. Lett.* **82**, 961 (2003).
20. T. Someya, J. Small, P. Kim, C. Nuckolls, J. T. Yardley, *Nano Lett.* **3**, 877 (2003).
21. J. Li *et al.*, *Nano Lett.* **3**, 929 (2003).
22. A. Goldoni, R. Larciprete, L. Petaccia, S. Lizzit, *J. Am. Chem. Soc.* **125**, 11329 (2003).
23. P. Qi *et al.*, *Nano Lett.* **3**, 347 (2003).
24. L. Valentini *et al.*, *Diamond Relat. Mater.* **13**, 1301 (2004).
25. J. P. Novak *et al.*, *Appl. Phys. Lett.* **83**, 4026 (2003).
26. Charge transfer from an analyte can potentially cause a capacitance response by changing the quantum capacitance of the nanotubes. We have simulated this chemical doping effect by applying to the substrate a small dc offset to the ac bias, which increases the charge in the SWNTs. By measuring the resulting capacitance and resistance responses, we calibrated the effect of a charge offset. For the vapors we have tested, most do not produce a measurable resistance response, and those that do, produce a resistance change that is much too small (based on this calibration) to account for the change in capacitance.
27. For an example, see the supplementary data available at Science Online.
28. B. M. Kim *et al.*, *Appl. Phys. Lett.* **84**, 1946 (2004).
29. We gratefully acknowledge financial support from the Homeland Security Advanced Research Projects Administration, the Office of Naval Research, and the Naval Research Laboratory Nanoscience Institute.

Supporting Online Material

www.sciencemag.org/cgi/content/full/307/5171/1942/DC1
SOM Text
Fig. S1

27 December 2004; accepted 1 February 2005
10.1126/science.1109128

Light Scattering to Determine the Relative Phase of Two Bose-Einstein Condensates

M. Saba,* T. A. Pasquini, C. Sanner, Y. Shin, W. Ketterle, D. E. Pritchard

We demonstrated an experimental technique based on stimulated light scattering to continuously sample the relative phase of two spatially separated Bose-Einstein condensates of atoms. The phase measurement process created a relative phase between two condensates with no initial phase relation, read out the phase, and monitored the phase evolution. This technique was used to realize interferometry between two trapped Bose-Einstein condensates without need for splitting or recombining the atom cloud.

The outstanding property of atoms in a Bose-Einstein condensate (BEC) is their coherence: They all have the same phase. This property became apparent when high-contrast interference between condensates was observed (1-3). Phase coherence between spatially separated

condensates has led to the observation of a host of phenomena, including Josephson oscillations (3, 4), number squeezing (5), and the transition from superfluid to Mott insulator (6).

The evolution of the phase is affected by external potentials acting on the atoms and has

been exploited for interferometric measures of gravity and other interactions (3, 7–9). Ideally, one could reach extreme interferometric sensitivity by coherently extracting atoms from two distant condensates and letting them interfere (10). So far, however, the relative phase of condensates has been measured only destructively, by taking an absorption image of interfering atomic waves.

Several methods have been considered to determine the relative phase of two separated atomic wavepackets spectroscopically by the scattering of light. In the simple case of a single atom delocalized in two separate wells, spontaneous photon scattering leaves the atom localized in one well, destroying the spatial coherence without giving any interferometric information (11, 12). On the other hand, selecting the frequency of the scattered photons makes it possible to retrieve interference from specially prepared wavepackets, like two spatially separated components moving on parallel trajectories (13). BECs offer the possibility of scattering many photons out

of the same coherent ensemble, affecting only a small fraction of the atoms in the condensates and providing an almost nondestructive measurement of the relative phase between the two condensates (14–16). Thus, light scattering could be used to compare the phase of two separate condensates at multiple subsequent times, realizing an interferometer with neither coherent splitting nor recombination of the wavepacket.

Even if the condensates are in states with poorly defined relative phase (such as the so-called Fock states, in which the atom number is well defined), they still interfere with each other. In this case, the relative phase is “created” in the measurement process by projecting the system on a coherent state with a well-defined phase (17–21).

We show that stimulated light scattering can be used to continuously sample the relative phase between two spatially separate BECs. The basis of our measurement is that the structure factor of two neighboring BECs shows interference fringes in momentum space (21). This interference can be pictured in a very direct way: Let us continuously impart some momentum \vec{q} to a fraction of the atoms in each condensate, so that they move parallel to the displacement of the two condensates. When the atoms from the first condensate reach the second one, the two

streams of atoms moving with momentum \vec{q} will overlap and interfere. The process can be rephrased as beating of two atom lasers originating from the two condensates. If the relative phase of the condensates is fixed, the total number of moving atoms depends on the value of the momentum q and oscillates sinusoidally with periodicity h/d as q is scanned (h is Planck’s constant and d is the displacement of the condensates). If instead the phase evolves in time and the momentum \vec{q} is fixed, the number of atoms in the moving stream will vary in time at the same rate as the relative phase.

The experimental tool used to impart a precise momentum to atoms in a BEC is Bragg scattering (22, 23). Two counterpropagating laser beams with wavevectors $\vec{k}_{1,2}$ hit the atoms so that, by absorbing a photon from one beam and reemitting it into the other one, the atoms acquire recoil momentum $\hbar(\vec{k}_2 - \vec{k}_1)$, provided that the energy difference between photons matches the atom recoil energy.

In our experiment (Fig. 1, A and B), two independent cigar-shaped BECs containing $\approx 10^6$ sodium atoms were prepared in a double-well optical dipole trap (8) and were

Department of Physics, MIT-Harvard Center for Ultracold Atoms, and Research Laboratory of Electronics, Massachusetts Institute of Technology, Cambridge, MA 02139, USA.

*To whom correspondence should be addressed. E-mail: msaba@mit.edu

Fig. 1. Interference of two atom lasers coupled out from two independent condensates. (A) Energy diagram of the two BECs (BEC I and BEC II) confined in an optical double-well trap. (B) Experimental scheme for continuous phase measurement. Two laser beams were applied to the condensates to decouple a few atoms from the trap. Detecting the rate of outcoupled atoms or the number of scattered photons gives a measurement of the relative phase between the condensates. The control coils generate magnetic field gradients that affect the frequency of interference oscillations. Gravity points down in this picture. (C to E) Absorption images showing the optical density of the atom clouds were taken from top after applying the Bragg beams (gravity points into the page). The thick shadows on the far left in each panel are the unresolved two condensates; to the right are the atoms that were continuously outcoupled and flew from left to right. High-contrast oscillations in the stream of outcoupled atoms are clearly visible. In the central picture (D), oscillations originated from the imbalance in the depth of the two wells. In (C), an additional magnetic field gradient of 1.15 G/cm was applied with the control coils; in (E), the gradient was -0.77 G/cm (with the positive direction pointing to the right). Images were taken after an additional 5 ms of time of flight, and the field of view in each picture is 1.35 mm \times 0.90 mm.

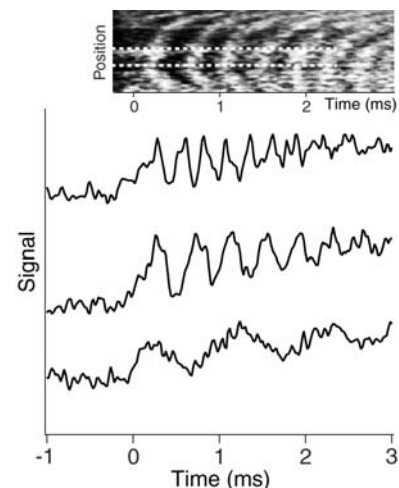
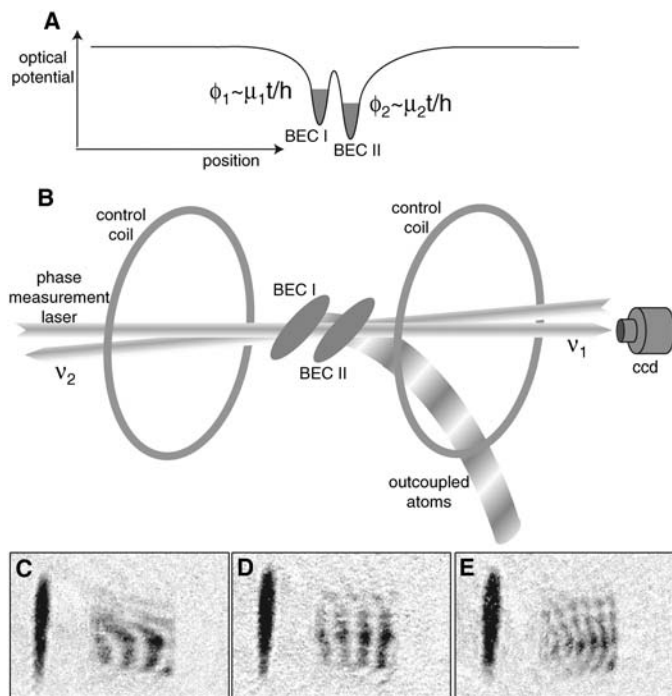


Fig. 2. Continuous optical readout of the relative phase of two condensates. In the upper panel is the optical signal image detected by streaking the CCD camera (24). The traces, offset vertically for clarity, are cross sections of the images (the central trace corresponds to the upper image integrated between the dashed lines). Bragg scattering starts at $t = 0$ when the second beam is turned on. The relative depth of the two wells was different for the three traces, generating a difference in the oscillation frequency. The overall slope on the traces was due to spontaneous Rayleigh scattering of the light from the atoms in the condensates. As the time went on, the condensates were depleted and the Rayleigh scattering was reduced. Excitations in the condensates appeared as tilted or curved fringes in the streak image; in such cases, we took cross sections from portions of the images where fringes were vertical and therefore the phase evolution was less perturbed.

illuminated with two counterpropagating Bragg beams to impart recoil momentum to a few atoms (24). The Bragg-scattered atoms flew away from the trap because the trap was shallower than the recoil energy. In the stream of outcoupled atoms (Fig. 1, C to E), the spatial modulations in the absorption images reflect temporal oscillations in the number of atoms outcoupled from the two condensates, implying a continuous evolution of the relative phase ϕ with time t at a rate $d\phi/dt = \Delta E/\hbar$, caused by the energy offset ΔE between the condensates. The three images were taken with different magnetic field gradients applied with the control coils. The difference in magnetic field between the two wells modified the energy offset ΔE and therefore affected the beat frequency $d\phi/dt$ of the two condensates. The fact that the fringes are not straight everywhere can be related to motional excitations in the condensates and the perturbing effect of the optical dipole potential on the time-of-flight trajectory of the atoms.

For each atom outcoupled from the condensate, a photon was transferred from one beam to the counterpropagating one. Therefore, all information contained in the stream of outcoupled atoms was also present

in the scattered light and could be gathered in real time by monitoring the intensity of one of the Bragg laser beams, instead of interrupting the experiment to illuminate atoms with a resonant laser for absorption imaging. The dynamics of the optical signal was measured with a charge-coupled device (CCD) camera in streaking mode, generating images with time on one axis and spatial information on the other (Fig. 2) (24). The intensity of the Bragg beam oscillated in time at a frequency controlled by the relative energy between the two wells. The oscillating signal built up during the first $\approx 250 \mu\text{s}$, this being the time required for the outcoupled atoms to travel from one condensate to the other one and start interference.

Interferometry between two trapped BECs was realized by continuous monitoring of their beat frequency. Figure 3 demonstrates the sensitivity of the interferometer to an applied external force (magnetic field gradient) and to the application of a potential difference between the two wells (dynamical Stark shift induced by increasing the laser power in one of the two wells).

We did not observe oscillation frequencies below 500 Hz. Short observation times and excitations could contribute to this, but there is

a fundamental limitation to the minimum measurable frequency due to interactions between atoms. If the phase stays (almost) constant for a long time, one of the two condensates can end up continuously amplifying or deamplifying the atoms outcoupled from the other one, causing asymmetric depletion of the condensates and therefore a difference in chemical potential, as large as a few $\hbar \times 100 \text{ Hz}$ in a few milliseconds under our experimental parameters. This is analogous to the inhibition of slow, large-amplitude Josephson oscillations in a nonlinear junction (25). If the relative phase is actively controlled, atoms can be coherently transferred from one well to the other, replenishing one of the two condensates without scrambling its phase; a method that could lead to a continuous atom laser (26).

The interferometric information contained in the beat frequency of two condensates is independent of the initial phase between the condensates and eliminates the need for coherent beam splitting (10). The present measurements already show a sensitivity below 100 Hz, limited by mechanical excitations that cause chirping of the frequency during the observation time and shot-to-shot variations. More fundamentally, the finite number of atoms in the condensates limits the number of Bragg-scattered photons and therefore the signal-to-noise ratio. No phase diffusion is expected during the measurement, the oscillations being continuously driven by the laser beams (27, 28). This is a general manifestation of the influence of measurement on a quantum system (29), similar to the quantum Zeno effect, where the time evolution is suppressed by repeated or continuous measurements.

A more versatile interferometric scheme can be obtained by applying two successive Bragg pulses to the pair of condensates and exploiting the fact that the optical phase readout allows comparison of subsequent measurements on the same pair of condensates. A first Bragg pulse lasting 1 ms determined a randomly varying relative phase between the two condensates at each realization of the experiment (Fig. 4B). A second Bragg pulse followed after allowing the two condensates to evolve for some delay (0.5 ms) and measured a relative phase again random at each shot

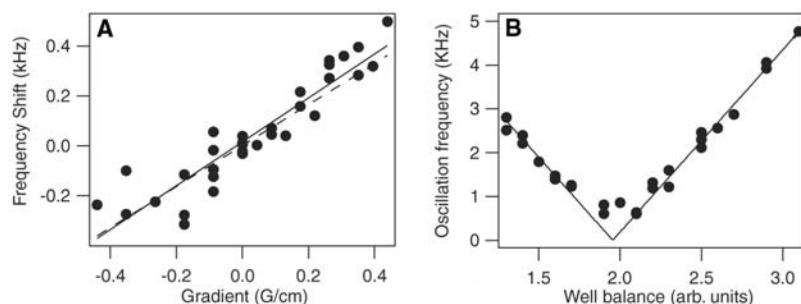


Fig. 3. Interferometry with two trapped BECs. (A) The two well depths were prepared offset by $\approx 0.53 \text{ kHz}$ in the absence of magnetic field gradients, and the shift of the beat frequency with respect to this initial value is plotted versus the applied magnetic field gradient. The beat frequency is determined from pictures similar to those in Fig. 2. The solid line is a linear fit to the data; the dashed line represents the frequency $\mu_B B' d/2\hbar$ expected for the evolution of the relative phase of the two condensates due to the difference in energy induced by the gradient (B' is the independently measured magnetic gradient, μ_B is half Bohr magneton corresponding to the magnetic moment of the atoms, and d is the displacement of the two condensates). (B) Beat frequency measured in the optical signal is shown as a function of the relative depth of the two potential wells. The well balance parameter is proportional to the difference in optical power used to create each of those wells and was controlled by the power in each of the two radio frequencies fed into the acousto-optical modulator. arb., arbitrary.

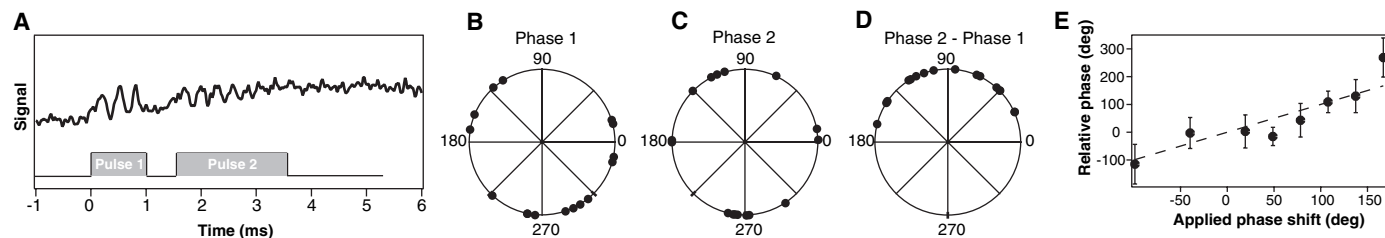


Fig. 4. Preparing a relative phase between two independent BECs with no initial phase relation. (A) The temporal trace of the Bragg beam intensity shown with the pulse sequence. (B) Phase of the oscillations recorded during the first pulse. (C) Phase during the second pulse. (D) Phase

difference between (B) and (C). (E) Phase difference between the oscillations in two pulses as a function of the phase shift applied during the evolution time between pulses. Each point is the average of several shots (between 3 and 10).

(Fig. 4C). Comparison with the phase measured in the first pulse shows that the two measurements were correlated (Fig. 4D). In other words, the first measurement established a definite relative phase between the two condensates that may not have had a defined phase before, and the second measurement verified that the condensates evolved with that particular phase during the interval between pulses.

Interferometry was demonstrated by putting an interaction time between the two pulses and changing the outcome of the second measurement. We briefly modified the energy offset between the two wells during the interval between the pulses, when the phase was not being observed. Figure 4E compares the measured phase shift with the value $\Delta E \Delta t / \hbar$ expected from an energy offset ΔE applied for a time Δt . The agreement between the prediction and the measurement demonstrates that the relative phase can be engineered by applying external forces to the atoms.

Active control of the phase opens interesting future perspectives: One could measure the light signal in real time and feed back the phase measurement into the control coils (or into the acousto-optical modulator that controls the two laser powers, creating the double-well potential), preparing the desired phase at the desired time. In principle, the uncertainty in the relative phase could even be squeezed by the feedback, allowing sub-shot noise interferometry (5, 10, 30).

Several physical interpretations of the experiment are possible besides the interference of two atom lasers. One is interference in momentum space (21): The zero-momentum component of the momentum distribution of the double condensate depends sinusoidally on the relative phase of the condensates and is probed with Doppler-sensitive spectroscopy (realized by Bragg scattering). Yet another point of view is that light scattering probes the excitation spectrum through the dynamical structure factor. The structure factor is phase-sensitive and shows interference fringes without requiring spatial overlap between the two condensates, as long as the excited states (after light scattering) have spatial overlap. This picture emphasizes that overlap between scattered atoms, as well as scattered photons, is crucial to our method: No phase information can be retrieved from two atomic wavepackets that scatter the same light but whose excited states are disconnected, like two condensates separated by a transparent glass wall.

The concept of beating atom lasers was previously exploited to measure spatial coherence in a single condensate (31) and for experiments done in optical lattices, where atoms outcoupled from a large vertical array of regularly spaced condensates interfered and their beating frequency measured gravity (3, 10). In this case, condensates were split coherently by raising the optical lattice poten-

tial. Coupling was established by tunneling of atoms between adjacent lattice sites and depended exponentially on the barrier shape, whereas the laser beams in our scheme established a coupling through a state delocalized over the barrier. In principle, larger barriers could be overcome by imparting larger momenta in the Bragg process. From the standpoint of precision interferometry, optical lattices have the advantage of a very well-known and controlled displacement between condensates, whereas the optical detection that we introduce here measures the beat frequency continuously and in real time, with accuracy not depending on the calibration of image magnification (3) or other disturbances affecting atoms during time of flight.

Our scheme to nondestructively measure the beat frequency of two previously independent condensates, thus establishing phase coherence, could permit us to couple condensates displaced by tens of microns on atom chips or in other microtraps, to explore Josephson oscillations, phase diffusion, and self-trapping. We have already demonstrated its potential in exploiting the phase coherence of BECs to create a novel type of atom interferometer.

References and Notes

1. M. R. Andrews *et al.*, *Science* **275**, 637 (1997).
2. D. S. Hall, M. R. Matthews, C. E. Wieman, E. A. Cornell, *Phys. Rev. Lett.* **81**, 1543 (1998).
3. B. P. Anderson, M. A. Kasevich, *Science* **282**, 1686 (1998).
4. F. S. Cataliotti *et al.*, *Science* **293**, 843 (2001).
5. C. Orzel, A. K. Tuchman, M. L. Fenselau, M. Yasuda, M. A. Kasevich, *Science* **291**, 2386 (2001).
6. M. Greiner, O. Mandel, T. Esslinger, T. W. Hänsch, I. Bloch, *Nature* **415**, 39 (2002).
7. S. Gupta, K. Dieckmann, Z. Hadzibabic, D. E. Pritchard, *Phys. Rev. Lett.* **89**, 140401 (2002).
8. Y. Shin *et al.*, *Phys. Rev. Lett.* **92**, 050405 (2004).
9. Y. J. Wang *et al.*, preprint available at <http://www.arxiv.org/abs/cond-mat/0407689> (2004).
10. M. A. Kasevich, *CR Acad. Sci. IV* **2**, 497 (2001).

11. C. CohenTannoudji, F. Bardou, A. Aspect, in *Laser Spectroscopy X*, M. Ducloy, E. Giacobino, Eds. (World Scientific, Singapore, 1992), p. 3.
12. K. Rażewski, W. Żakowicz, *J. Phys. B* **25**, L319 (1992).
13. B. Dubetsky, P. R. Berman, *J. Mod. Opt.* **49**, 55 (2002).
14. J. Javanainen, *Phys. Rev. A* **54**, 4629(R) (1996).
15. A. Imamoglu, T. A. B. Kennedy, *Phys. Rev. A* **55**, 849(R) (1997).
16. J. Ruostekoski, D. F. Walls, *Phys. Rev. A* **56**, 2996 (1997).
17. J. Javanainen, S. M. Yoo, *Phys. Rev. Lett.* **76**, 161 (1996).
18. M. Naraschewski, H. Wallis, A. Schenzle, J. I. Cirac, P. Zoller, *Phys. Rev. A* **54**, 2185 (1996).
19. J. I. Cirac, C. W. Gardiner, M. Naraschewski, P. Zoller, *Phys. Rev. A* **54**, 3714(R) (1996).
20. Y. Castin, J. Dalibard, *Phys. Rev. A* **55**, 4330 (1997).
21. L. Pitaevskii, S. Stringari, *Phys. Rev. Lett.* **83**, 4237 (1999).
22. M. Kozuma *et al.*, *Phys. Rev. Lett.* **82**, 871 (1999).
23. J. Stenger *et al.*, *Phys. Rev. Lett.* **82**, 4569 (1999).
24. Information on materials and methods is available on Science Online.
25. A. Smerzi, S. Fantoni, S. Giovanazzi, S. R. Shenoy, *Phys. Rev. Lett.* **79**, 4950 (1997).
26. A. P. Chikkatur *et al.*, *Science* **296**, 2193 (2002).
27. M. Lewenstein, L. You, *Phys. Rev. Lett.* **77**, 3489 (1996).
28. J. Javanainen, M. Wilkens, *Phys. Rev. Lett.* **78**, 4675 (1997).
29. J. A. Wheeler, W. H. Zurek, *Quantum Theory and Measurement* (Princeton Univ. Press, Princeton, NJ, 1983).
30. J. M. Geremia, J. K. Stockton, H. Mabuchi, *Science* **304**, 270 (2004).
31. I. Bloch, T. W. Hansch, T. Esslinger, *Nature* **403**, 166 (2000).
32. This work was funded by the Army Research Office, the Defense Advanced Research Projects Agency, NSF, the Office of Naval Research, and NASA. M.S. acknowledges additional support from the Swiss National Science Foundation and C.S. from the Studienstiftung des deutschen Volkes. We thank G. Jo for experimental assistance, A. Schirotzek for contributions in the early stage of the work, and M. Zwierlein for a critical reading of the manuscript. We are indebted to A. Leanhardt for stimulating suggestions that initiated this research and insightful comments on the experiment and the manuscript.

Supporting Online Material

www.sciencemag.org/cgi/content/full/307/5717/1945/DC1

Materials and Methods

16 December 2004; accepted 3 February 2005
10.1126/science.1108801

Cool La Niña During the Warmth of the Pliocene?

R. E. M. Rickaby and P. Halloran

The role of El Niño–Southern Oscillation (ENSO) in greenhouse warming and climate change remains controversial. During the warmth of the early-mid Pliocene, we find evidence for enhanced thermocline tilt and cold upwelling in the equatorial Pacific, consistent with the prevalence of a La Niña–like state, rather than the proposed persistent warm El Niño–like conditions. Our Pliocene paleothermometer supports the idea of a dynamic “ocean thermostat” in which heating of the tropical Pacific leads to a cooling of the east equatorial Pacific and a La Niña–like state, analogous to observations of a transient increasing east-west sea surface temperature gradient in the 20th-century tropical Pacific.

In 1976, the equatorial Pacific, potentially driven by anthropogenic warming, switched from a weak La Niña state to one in which

El Niño occurs with greater frequency and intensity (1). For the current climate system, El Niño years are warmer and La Niña years are cooler (2). In the future, more persistent El Niño could amplify global warming. Determining what drives ENSO and how

Department of Earth Sciences, University of Oxford, Parks Road, Oxford OX1 3PR, UK.